

AD-A282 222



**Dynamic Sine Wave
Response Measurements of CRT Displays
Using Sinusoidal Counterphase Modulation
(Reprint)**

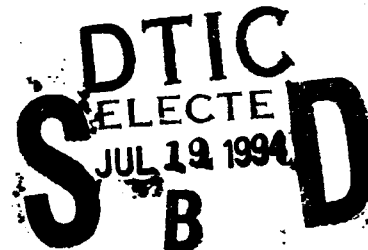
By

Robert W. Verona
Howard H. Beasley
John S. Martin
Victor Klymenko

UES, Incorporated

and

Clarence E. Rash
Aircrew Health and Protection Division



20P8 94-22459

April 1994

94 7 18 013

DTIC QUALITY INSPECTED 1

Approved for public release; distribution unlimited.

United States Army Aeromedical Research Laboratory
Fort Rucker, Alabama 36362-0577

Notice

Qualified requesters

Qualified requesters may obtain copies from the Defense Technical Information Center (DTIC), Cameron Station, Alexandria, Virginia 22314. Orders will be expedited if placed through the librarian or other person designated to request documents from DTIC.

Change of address

Organizations receiving reports from the U.S. Army Aeromedical Research Laboratory on automatic mailing lists should confirm correct address when corresponding about laboratory reports.


Disposition

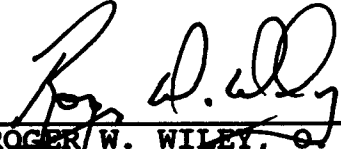
Destroy this document when it is no longer needed. Do not return it to the originator.

Disclaimer


The views, opinions, and/or findings contained in this report are those of the author(s) and should not be construed as an official Department of the Army position, policy, or decision, unless so designated by other official documentation. Citation of trade names in this report does not constitute an official Department of the Army endorsement or approval of the use of such commercial items.

Reviewed:


RICHARD R. LEVINE
LTC, MS
Director, Aircrew Health
and Performance Division


ROGER W. WILEY, O. D., Ph.D.
Chairman, Scientific
Review Committee

Released for publication:


DAVID H. KARNEY
Colonel, MC, SFS
Commanding

Unclassified

SECURITY CLASSIFICATION OF THIS PAGE

REPORT DOCUMENTATION PAGE

Form Approved
OMB No. 0704-0188

1a. REPORT SECURITY CLASSIFICATION Unclassified		1b. RESTRICTIVE MARKINGS	
2a. SECURITY CLASSIFICATION AUTHORITY		3. DISTRIBUTION/AVAILABILITY OF REPORT Approved for public release; distribution unlimited	
2b. DECLASSIFICATION/DOWNGRADING SCHEDULE		5. MONITORING ORGANIZATION REPORT NUMBER(S)	
4. PERFORMING ORGANIZATION REPORT NUMBER(S) USAARL Contract Report No. 94-22		7a. NAME OF MONITORING ORGANIZATION U.S. Army Medical Research, Development, Acquisition and Logistics Command(Provisional)	
6a. NAME OF PERFORMING ORGANIZATION U.S. Army Aeromedical Research Laboratory	6b. OFFICE SYMBOL (If applicable) SGRD-UAS-VS	7b. ADDRESS (City, State, and ZIP Code) Fort Detrick Frederick, MD 21702-5012	
6c. ADDRESS (City, State, and ZIP Code) P.O. Box 620577 Fort Rucker, AL 36362-0577		9. PROCUREMENT INSTRUMENT IDENTIFICATION NUMBER	
8a. NAME OF FUNDING/SPONSORING ORGANIZATION	8b. OFFICE SYMBOL (If applicable)	10. SOURCE OF FUNDING NUMBERS	
8c. ADDRESS (City, State, and ZIP Code)		PROGRAM ELEMENT NO. 0602787A	PROJECT NO. 3E1672 787A879
		TASK NO. BG	WORK UNIT ACCESSION NO. 164
11. TITLE (Include Security Classification) (U) Dynamic Sine Wave Response Measurements of CRT Displays Using Sinusoidal Counterphase Modulation (Reprint)			
12. PERSONAL AUTHOR(S) Robert W. Verona, Howard H. Beasley, John S. Martin, Victor Klymenko, and Clarence E. Rash			
13a. TYPE OF REPORT	13b. TIME COVERED FROM _____ TO _____	14. DATE OF REPORT (Year, Month, Day) 1994 April	15. PAGE COUNT 10
16. SUPPLEMENTARY NOTATION Presented and published in proceedings of SPIE's 1994 Technical Symposium on Helmet Mounted Displays, Volume 2218; Orlando, FL; 4-8 Apr 1994			
17. COSATI CODES		18. SUBJECT TERMS (Continue on reverse if necessary and identify by block number)	
FIELD	GROUP	SUB-GROUP	
20	06		
23	02		
19. ABSTRACT (Continue on reverse if necessary and identify by block number)			
<p>The current practice of basing the performance of cathode ray tube (CRT) displays on static image quality figures-of-merit fails to provide a valid assessment of a display's ability to reproduce real-world scenes where there is relative motion within the scene or between the sensor and scene. Techniques which provide assessment of a display's capability to reproduce spatial information in a dynamic environment are needed. One technique based on response to sinusoidal counterphase modulation is presented.</p>			
20. DISTRIBUTION/AVAILABILITY OF ABSTRACT <input checked="" type="checkbox"/> UNCLASSIFIED/UNLIMITED <input type="checkbox"/> SAME AS RPT. <input type="checkbox"/> DTIC USERS		21. ABSTRACT SECURITY CLASSIFICATION Unclassified	
22a. NAME OF RESPONSIBLE INDIVIDUAL Chief, Science Support Center		22b. TELEPHONE (Include Area Code) (205) 255-6907	22c. OFFICE SYMBOL SGRD-UAX-SI

Dynamic Sine Wave Response Measurements of CRT Displays Using Sinusoidal Counterphase Modulation

**Robert W. Verona
Howard H. Beasley
John S. Martin
Victor Klymenko**

**UES, Inc.
Fort Rucker, Alabama 36362**

and

Clarence E. Rash

**U.S. Army Aeromedical Research Laboratory
Fort Rucker, Alabama 36362**

ABSTRACT

The current practice of basing the performance of cathode ray tube (CRT) displays solely on static image quality figures-of-merit fails to provide a valid assessment of a display's ability to reproduce real-world scenes where there is relative motion within the scene or between the sensor and scene. Techniques which provide assessment of a display's capability to reproduce spatial information in a dynamic environment are needed. One technique based on response to sinusoidal counterphase modulation is presented.

1. INTRODUCTION

A scene reproduced by an imaging system can be classified as static (passive) or dynamic (active). The term static implies there are no temporal characteristics attributed to the scene. Usually this means there is no motion within the scene. The term dynamic is used when relative motion exists either within the scene or between the sensor and the scene. By function, imaging systems always are dynamic in nature, i.e., there is always some time constant associated with the imaging process. When the scene is static, an imaging system will produce an image of the scene unaffected by motion (time) related interactions. However, when imaging a dynamic scene, the sensor's and display's inherent temporal characteristics in conjunction with those of the scene become important factors in the fidelity of the reproduced scene. For these reasons, techniques used to assess an imaging system's capability to faithfully reproduce a scene must reflect these temporal characteristics.

By convention, imaging systems have been characterized with static assessment techniques. This most likely is the result of experience in early photography where the film "speed" was very slow and objects in the scene were required to remain motionless. However, in imaging systems which use displays such as cathode ray tubes (CRTs), interactions between the temporal characteristics of the scene and the sensor are important factors in the display's resultant image quality. In spite of this fact, CRT display performance historically has been characterized using the same static assessment techniques as used with passive optical systems.¹ This static assessment approach provides an inadequate assessment of a CRT's performance for conditions where there is relative motion within the targeting scene or between the observer and the scene. This misrepresentation is a result of the interaction of the relative motion and the inherent temporal characteristics of the sensor and CRT. Temporal characteristics of the CRT include phosphor persistence, horizontal scan rate, vertical refresh rate, and amplifiers' bandwidths.

Head-mounted and head-tracked imaging systems, which employ CRT-based display technology, are particularly vulnerable to image degradation in dynamic imaging scenarios. The relative motion between an object in the imaging system's field-of-regard (FOR) and the observer's line-of-sight (LOS) can be hundreds of degrees per second. Self-contained night vision devices, such as night vision goggles (NVGs), display moving images at angular velocities that match those of the head. Velocities associated with head-tracked imaging systems are limited by the temporal response of the tracker and turret systems. Typically, 120 degrees/second is considered to be about the 95th percentile velocity for both azimuth and elevation movements, and 30 degrees/seconds is considered to be about the 50th percentile.²

The movement rates of concern are applicable to both continuous observation (tracking) and glances. The observer typically reduces head movement rates when there is a noticeable degradation in image quality that can be minimized by slowing the relative movement under the observer's control. Even when the objective is to glance in another direction, where the information between the initial and subsequent direction of gaze are of no interest to the observer, the duration of gaze motion is determined by cognitive factors rather than just the mechanics of orienting the head/eyes in the direction of interest. At suprathreshold conditions, the motion induced image quality reduction may be of little consequence. However, when the sensor, display, and observer are functioning near their operating limits, even a modest reduction in image quality may be of considerable consequence but not readily apparent to the observer. An electro-optical system which meets performance requirements during a static bench test actually may provide much less scene information than expected when in actual use.

Contrast is one physical metric commonly used by both vision scientists and engineers for describing image quality. Contrast, generally defined as the difference between the brightest and darkest regions of a scene, can be expressed in a number of ways, some of which are more appropriate than others for specific applications. For CRT displays, modulation contrast, or Michelson contrast, is often the most appropriate metric for describing their capacity to convey relative luminance. Modulation contrast (M_c), defined as

$$M_c = (L_{\max} - L_{\min}) / (L_{\max} + L_{\min}),$$

where L_{\max} is the maximum luminance and L_{\min} is the minimum luminance, is a common figure-of-merit used to quantify a display's image quality.³ Modulation contrast can be related to the integer number of gray scales an analog display is capable of reproducing. For CRT displays, discriminable gray scales usually are defined as the levels of luminance differing by the square root of two. The relationship between gray scales and modulation contrast associated with this definition is depicted in Figure 1.

The ability of a display to reproduce contrast is spatial frequency dependent, and as we shall see also is temporal frequency dependent. Spatial frequency refers to the rate of luminance change over space, typically expressed as the number of sine wave cycles per display width. Temporal frequency refers to the rate of luminance change over time, which is expressed in Hertz. When modulation contrast values are measured for a specific display, expressed as ratios to the input modulation, and plotted as a function of spatial frequency, the resulting curve (Figure 2) is referred to as the display's modulation transfer function (MTF). For a static CRT image, the MTF, measurable by any of a number of available techniques,⁴ can be interpreted as the MTF for the scenario where the relative motion within the scene is zero.

The modulation contrast values and resulting MTFs of a static image and one with a relative motion of 30 degrees/second can be quite different for a CRT display. For a static image, the modulation contrast values for high spatial frequencies normally are lower than for low spatial frequencies. Similarly, the modulation contrast values for high relative velocities normally are lower than for low relative velocities. The modulation contrast value of a high velocity, high spatial frequency object easily can fall below the human visual threshold while the same high spatial frequency object at rest can have a value above this threshold. A preliminary model which describes a family of MTF curves, with a separate curve for different values of relative velocity, has

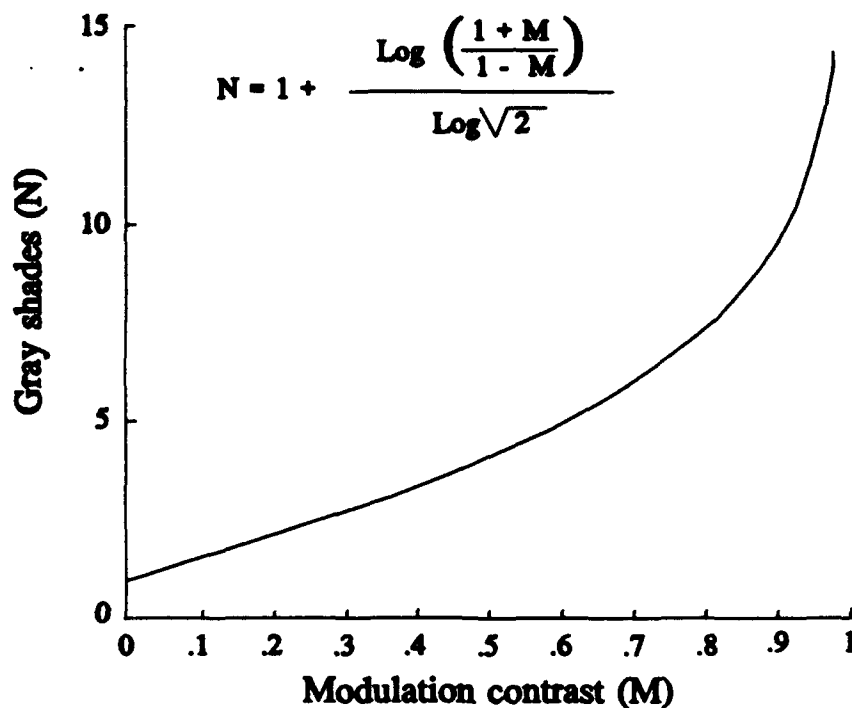


Figure 1. Relationship between gray scales and modulation contrast.

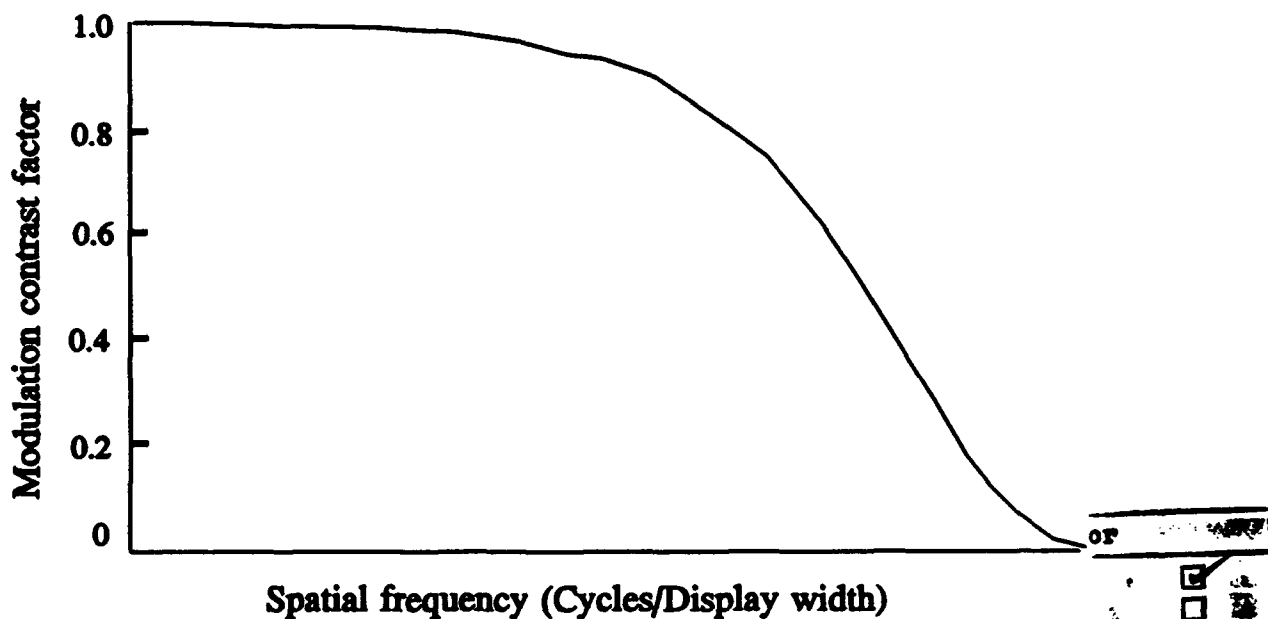


Figure 2. Typical modulation transfer function curve.

By _____	
Distribution/... # _____	
Availability Codes	
Dist	Avail and/or Special
A-1	

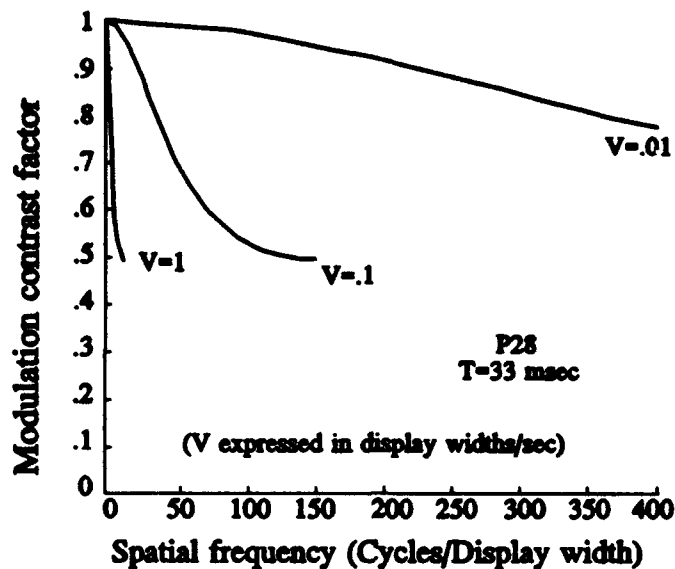


Figure 3. Modeled dynamic modulation transfer curves.

been developed for CRT displays by Rash and Becher.⁵ The model predicts reductions in MTF resulting from the interaction of target/scene relative motion and the display's temporal characteristics of scan rate and phosphor persistence. Figure 3 depicts a modeled family of curves for a P-28 phosphor (70 ms, 10%) in a CRT display with a vertical frame period of 33 ms; three curves which are representative of three relative velocities are shown.

In order to accurately describe the performance of CRT displays used in dynamic environments such as driving, pilotage, or target acquisition systems, these displays must be characterized for dynamic images. Measuring the display's static performance and expecting it to be representative of its performance for moving imagery is unrealistic. The actual performance may be degraded significantly from the inflated expectations based on the static assumption. The loss of gray scale and high spatial frequency information may lead to dire consequences. As an example, during the early design phase of the AH-64 Apache attack helicopter, an incident was reported where the test pilot, viewing imagery on the Integrated Helmet and Display Sighting System (IHADSS) helmet-mounted display, lost sight of some small branches in his field-of-regard (FOR) during a nap-of-the-earth (NOE) flight. This resulted in a blade strike and damage to the aircraft. The head-coupled display with its P-1 phosphor was suspected to be the source of the problem. The 24-millisecond (ms) persistence (10%) of the P-1 phosphor did not have the temporal response required to display the high spatial frequency branches during moderate head movements. When the CRT phosphor was replaced by a lower persistence P-43 phosphor (1.2 ms, 10%), the branches were visible under the same conditions. The static MTF of displays with P-1 and P-43 phosphors were similar, but the dynamic characteristics of the phosphors made the difference between success and failure.

Verona⁴ has suggested the most accurate method of obtaining the static MTF of a CRT display is the discrete sine wave frequency response method. This method involves generating a sine wave modulation pattern at a selected low spatial frequency (e.g., 2-3 cycles/display width) on the CRT, scanning the pattern using a scanning microphotometer, and calculating the modulation contrast ratio value. While maintaining a constant modulation input signal, this procedure is repeated for ever increasing spatial frequencies until the modulation

contrast approaches zero (typically less than 0.05). Plotting these values as a function of spatial frequency provides the static MTF curve—to be thought of as the first of a series of dynamic MTF curves, i.e., for a relative velocity value of zero. To fully characterize the display, additional dynamic MTF curves need to be developed for other velocity values. Two techniques, the counterphase modulation and the drifting sine wave techniques, can be used to obtain these curves. The drifting sine wave technique is based on spatial sinusoidal patterns which continuously change in phase, resulting in an apparent movement of the spatial patterns on the display. The counterphase modulation technique involves placing multiple spatial frequencies on the display (one at a time) and having the white and black portions of each cycle alternate between their maximum or minimum intensities (contrast reversal). The counterphase modulation technique is described in this paper.

2. DISPLAY SETUP

To characterize a CRT display, the operating parameters of the display must first be set for the anticipated operating environment. This is true regardless of the technique used to measure the display's performance. The signal levels, line rate, focus, peak luminance (brightness), contrast, and image size/aspect ratio are some of the more important operating parameters that can influence the display's performance. The video test signals should match the anticipated operating video levels and timing. RS-170A NTSC or RS-343 standards are appropriate for most applications. If the display is to be used in more than one environment, for example under both day and night conditions, then two sets of performance measurements are appropriate, one set for day viewing and the other for night viewing conditions. Similarly for the line rate, if the display will be used to present both 875- and 525-line video, it must be tested at both line rates. Four sets of data would be required if both line rates are used under both day and night conditions.

For the data reported here, a Conrac model SNA 14/N monitor operating with RS-170A NTSC (525-line rate) video was evaluated under simulated night conditions (in a fully darkened laboratory). The monitor was fitted successively with CRTs with P-44 (1.2 ms, 10%) and P-1 (24 ms, 10%) phosphors. Following adjustment of focus and aspect ratio using the manufacturer's recommended procedures, the display's brightness and contrast were set using the following procedure.

First, a predetermination of peak brightness was made. For the simulated night environment, a value of 15 footlamberts was chosen. For a desired white/black ratio of 100:1, this required the black level luminance to be 0.15 footlambert. Brightness and contrast controls were adjusted to their minimum settings (fully counterclockwise). Inputting a low spatial frequency square wave 1-volt peak-to-peak video signal, the brightness control was increased until the raster was just barely visible. The contrast control then was advanced to a setting which produced a 15 footlamberts luminance value at the peak of the pattern (maximum video level). The black level luminance (minimum video level) was examined to see if the 0.15 footlambert value was present. As required, the brightness and contrast controls were adjusted alternately to achieve the 100:1 ratio. The luminance values associated with the minimum and maximum video levels were measured using a Minolta 1-degree luminance meter. These values were 0.15 and 15 footlamberts, respectively.

3. COUNTERPHASE MODULATION TECHNIQUE

This technique attempts to take advantage of the flexible and robust nature of the computer as a signal generating imaging source. With such a configuration, software can be written to generate custom test patterns for static or dynamic presentations on the display. The modulation contrast of the patterns can be measured photometrically as the patterns vary in spatial and temporal frequency.

The displays used in the evaluation were driven by computer generated static and dynamic sine wave spatial patterns with the long dimension of the pattern at a 90° angle (vertical) to the display's scan line structure. For the static case, spatial frequency sine wave patterns of selected frequencies were generated and

presented on the display. The modulation contrast measurements were made using the peak and trough luminance values obtained from the resulting display image. For the dynamic case, the spatial sine wave patterns also were modulated temporally at selected sinusoidal frequencies. One temporal cycle of the stimulus consisted of the luminance at a position on the display changing from its brightest value to its darkest value and back to its brightest value (counterphase). As a result, the luminance variations on the display were sinusoidal in both spatial and temporal domains.

This temporal sinusoidal test stimulus is different from a square wave counterphase flicker stimulus where the luminance at a point on the display is alternated in a square wave fashion with abrupt transitions from bright to dark. The sinusoidal variation provides a purer stimulus since there is a strong tendency for the turn-on in the square wave input to overshoot in luminance. This overshoot causes the modulation to be exaggerated, i.e., the peak luminance for high spatial frequencies becomes greater than would normally be caused by an input signal within the bandwidth limitations of the display. This overshoot easily can be interpreted during modulation transfer function analysis as an improved high frequency response when, in fact, it is an artifact of the display's response to the fast rise time stimulus and subsequent overshoot. This same result is not apparent when the turn-off portion of the square wave stimulus is analyzed.

A pictorial diagram of the experimental setup is presented in Figure 4. Stimulus generation was performed using a computer graphics workstation which was linked to a video scan converter. Measurement of the resulting display peak and trough luminances, which were used to calculate the modulation contrast values, was accomplished using a combination of collection optics, a photomultiplier tube (PMT), a high voltage supply, electronic filters, and a digital storage oscilloscope.

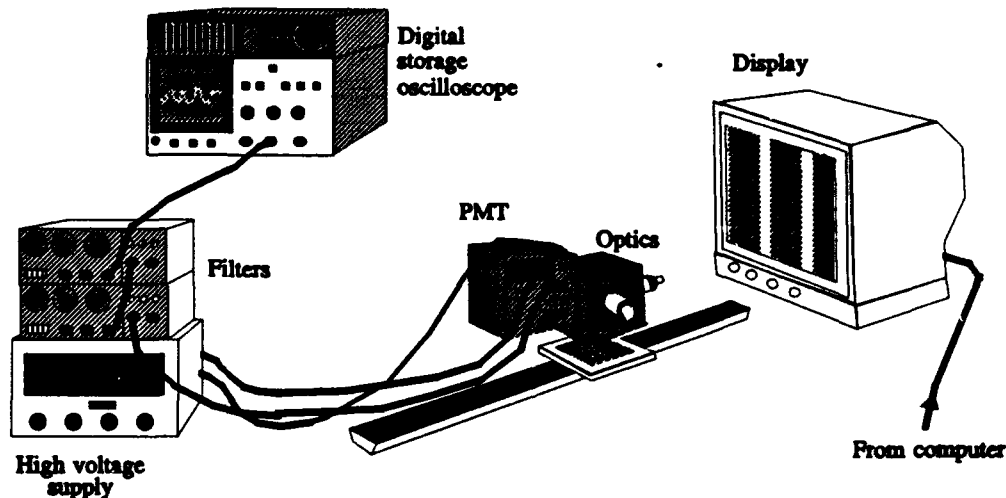


Figure 4. Pictorial diagram of the experimental setup.

Stimulus patterns were generated with a Hewlett-Packard model HP-98731 Turbo-SRX computer graphics workstation. The output of the computer was fed to a Folsom Research, Inc. model 8910 color graphics converter which produced a RS-170A NTSC video signal. This video signal was used to drive the display under evaluation. The software which produced the stimulus patterns was written in the C programming language running in an UNIX environment. Except for aliasing effects, the patterns theoretically could be generated at any desired spatial frequency and presented at any temporal frequency at or below 30 Hertz. For the evaluation presented here, combinations of the spatial and temporal frequencies presented in Table 1 were used. By convention, contrast measurements were not made for combinations beyond the point where the modulation contrast (M_c) dropped off to less than 5 percent (0.05) or display artifacts were encountered.

Table 1.

Spatial and temporal frequencies

Spatial (Cycles/display width)	Temporal (Hertz)
3.6, 7.1, 10.7, 14.2, 17.8, 21.3, 28.4, 32.0, 35.6, 42.7, 64.0, 71.1, 85.3, 106.0, 128.0, 142.2, 160.0, 177.8	0, 1.875, 3.75, 5.0, 7.5, 10.0

The physical and electrical characteristics of the collection optics, PMT, and high voltage supply (which together function as a photometer) are critical to the interpretation of the measurements. A slit aperture is recommended. Its width should be approximately 10 times smaller than the highest spatial frequency measured in the object plane and its length should cover at least approximately 5 display scan lines. A 25 X 8000 micron width to length ratio was used for this evaluation. The objective lens power determines the effective width and length in the objective plane. A 5X microscope lens was used to give an effective 5 X 1600 micron measurement slit on the display screen. If the effective slit width is too large, the modulation amplitude measurements will be artificially low. If the slit width is too small, the luminance signal level will be low and noisy.

A Gamma Scientific, Inc. model DR-2 digital radiometer, model D-46A PMT assembly with 4 MHz high frequency amplifier, and model 700-10 photometric microscope with a 25 X 8000 micron slit were used to convert the spatial and temporal luminance values into an electrical signal which was measured using a Tektronix model 2440 digital storage oscilloscope. The model DR-2 radiometer was used only as a source of high voltage for the PMT and a high voltage value of 700 volts was used. The output of the high frequency amplifier of the PMT was filtered by two Frequency Devices, Inc. model 901F electronic filters before being fed to the oscilloscope. The filters, connected in series, acted as a low pass filter with a cutoff frequency of 35 Hertz and provided 40 dB of gain. The temporal response of the photometer is very critical for the dynamic measurements. The limited range of response speeds typically encountered in off-the-shelf photometers is inadequate for reliable dynamic measurements. Therefore, the video or high frequency output of the photometer was used. The electronic filters provided amplification and filtered out high frequency noise, improving the signal-to-noise ratio. The output of the filter was displayed on a digital oscilloscope.

To evaluate the static case, zero Hertz temporal frequency, contrast measurements were made over the spatial frequency range of approximately 3 cycles per display width to the cutoff frequency, where the modulation contrast dropped off to less than 5 percent. For each spatial frequency, a peak of the sine wave was positioned in front of the photometer and the resulting maximum output was read from the display of the oscilloscope and recorded. Then a trough of the sine wave was positioned and the resulting minimum output was read and recorded. These data, when used to calculate the contrast values, represent the sine wave response of the display for the static image condition.

For the dynamic measurements, a temporal frequency was selected and an input signal was applied to the display at each spatial frequency. For each spatial frequency, the photometer output signal was acquired using the storage oscilloscope. From the digitized waveform, the peak and trough values were obtained and used to calculate the modulation contrast value. This procedure was repeated for each temporal frequency.

Modulation transfer ratios were calculated from the input and output modulation contrast data for all spatial and temporal frequency combinations and presented as MTF curves.

4. PERFORMANCE DATA

MTF curves for the P-44 and P-1 displays are presented in Figures 5 and 6, respectively. The family of curves for the P-44 phosphor did not show any significant differences between the display's performance for the various temporal frequencies tested. However, the P-1 curves showed significant differences for the 7.5 and 10.0 Hz temporal frequencies.

The lack of definition between the dynamic MTF curves for the P-44 phosphor was expected since the 1.2 ms persistence value characterizes P-44 as a medium-short persistence (fast) phosphor. The performance of this phosphor did not noticeably degrade as the temporal frequency was increased. For the P-1 phosphor with its 24 ms (medium) persistence, the dynamic MTF curves for 7.5 and 10.0 Hz were significantly different from the other temporal frequencies. Although not statistically significant, the trend in the contrast modulation values and resulting MTF curves was that of having consistently greater values for the lowest temporal frequency (1.875 Hz) than for the static condition (0 Hz). This was true for both display phosphors. It is believed this is a result of a low-frequency response defect present in many AC-coupled video amplifiers.⁶ (Note: The same drive electronics was used for both CRT phosphors.)

5. SUMMARY

The sinusoidal counterphase modulation method proved capable of assessing a display's dynamic performance. This was demonstrated for two phosphor displays, one (P-44) for which no degradation was expected and one (P-1) for which degradation due to motion has been documented. However, this technique exhibited several limitations which reduced its desirability. First, the technique was very tedious and time consuming. Considerable patience and effort were required in reading the peak and trough values from the

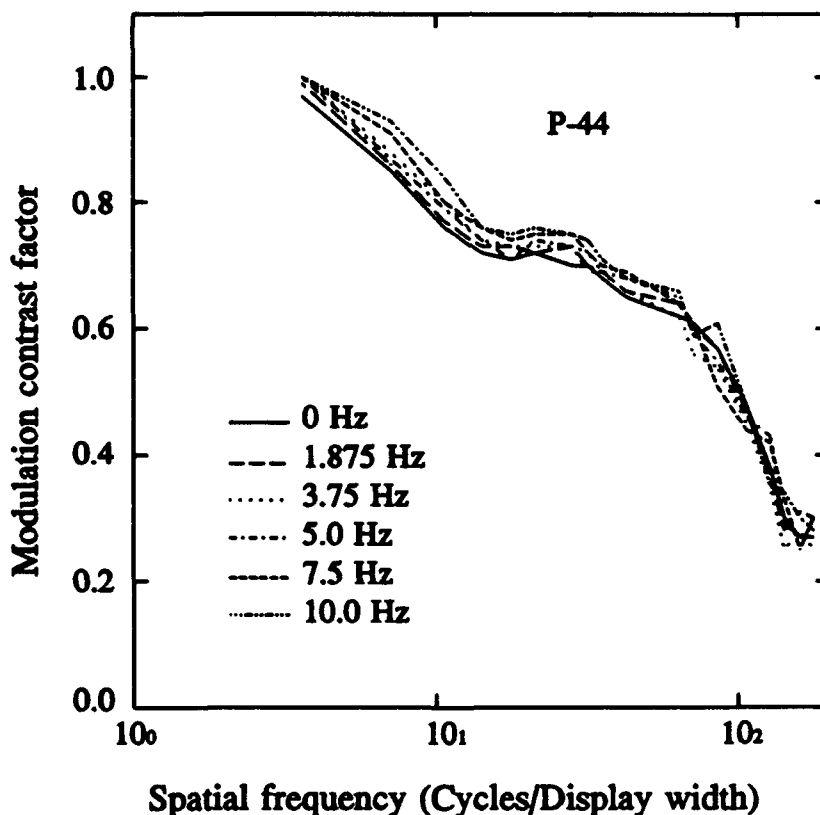


Figure 5. MTF curves for P-44 phosphor display.

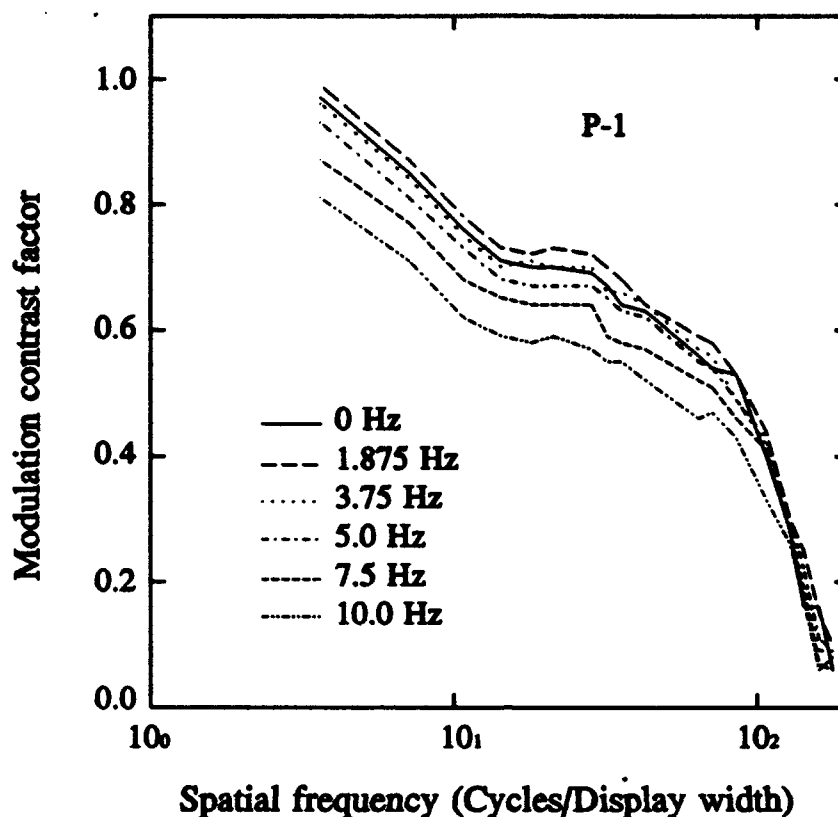


Figure 6. MTF curves for P-1 phosphor display.

storage oscilloscope waveforms. The average time required to complete measurements for the spatial and temporal frequency combinations in Table 1 was approximately 2-1/2 hours. Second, while the use of the computer graphics workstation provided flexibility in the generation of spatial and temporal patterns, the conversion of the workstation's RGB digital output into 525-line rate video resulted in a test signal which was nonuniform in its modulation. This limitation required additional measurements and had to be compensated for in the MTF calculations. In addition, this signal contained a beat frequency which caused some difficulty in the ability to measure waveforms accurately for the higher spatial frequencies. In spite of these limitations, the sinusoidal counterphase modulation technique provides a functional approach to assessing a CRT display's performance in the temporal domain.

6. ACKNOWLEDGMENTS

The authors wish to thank Mr. Udo Volker Nowak for his invaluable assistance in the preparation and review of this paper and Mr. Bob Dillard for his technical assistance.

This work is supported by the U.S. Army Medical Research and Development Command under Contract No. DAMD17-91-C-1081.

7. DISCLAIMER

The views, opinions and or findings contained in this paper are those of the authors and should not be construed as an official Department of the Army position, policy, or decision unless so designated by other official documentation.

8. REFERENCES

1. C.E. Rash and R.W. Verona, "Temporal aspects of electro-optical imaging systems," *Imaging Sensors and Displays*, Proceedings SPIE, Vol. 765, pp. 22-25, 1987.
2. R.W. Verona, C.E. Rash, W.R. Holt, and J.K. Crosley, "Head movements during contour flight," U.S. Army Aeromedical Research Laboratory, Fort Rucker, AL. USAARL Report No. 87-1, 1986.
3. H.L. Task, "An evaluation and comparison of several measures of image quality for television displays," Wright-Patterson Air Force Base, OH: Aerospace Medical Research Laboratory, AMRL TR-79-7-9, 1979.
4. R.W. Verona, "Comparison of CRT display measurement techniques." in *Helmet Mounted Displays III*, Proceedings SPIE, Vol. 1695, pp. 117-127, 1992.
5. C.E. Rash and J. Becher, "Analysis of image smear in CRT displays due to scan rate and phosphor persistence," U.S. Army Aeromedical Research Laboratory, Fort Rucker, Fort Rucker, AL. USAARL Report No. 83-5, 1982.
6. F.E. Terman, Electronic and radio engineering, McGraw-Hill Book Company, Inc., New York, 1955.

Initial distribution

Commander, U.S. Army Natick Research,
Development and Engineering Center
ATTN: SATNC-MIL (Documents
Librarian)
Natick, MA 01760-5040

Library
Naval Submarine Medical Research Lab
Box 900, Naval Sub Base
Groton, CT 06349-5900

Chairman
National Transportation Safety Board
800 Independence Avenue, S.W.
Washington, DC 20594

Executive Director, U.S. Army Human
Research and Engineering Directorate
ATTN: Technical Library
Aberdeen Proving Ground, MD 21005

Commander
10th Medical Laboratory
ATTN: Audiologist
APO New York 09180

Commander
Man-Machine Integration System
Code 602
Naval Air Development Center
Warminster, PA 18974

Naval Air Development Center
Technical Information Division
Technical Support Detachment
Warminster, PA 18974

Commander
Naval Air Development Center
ATTN: Code 602-B
Warminster, PA 18974

Commanding Officer, Naval Medical
Research and Development Command
National Naval Medical Center
Bethesda, MD 20814-5044

Commanding Officer
Armstrong Laboratory
Wright-Patterson
Air Force Base, OH 45433-6573

Deputy Director, Defense Research
and Engineering
ATTN: Military Assistant
for Medical and Life Sciences
Washington, DC 20301-3080

Director
Army Audiology and Speech Center
Walter Reed Army Medical Center
Washington, DC 20307-5001

Commander, U.S. Army Research
Institute of Environmental Medicine
Natick, MA 01760

Commander/Director
U.S. Army Combat Surveillance
and Target Acquisition Lab
ATTN: SFAE-IEW-JS
Fort Monmouth, NJ 07703-5305

Commander
USAMRDALC
ATTN: SGRD-UMZ
Fort Detrick, Frederick, MD 21702-5009

Commander
U.S. Army Health Services Command
ATTN: HSOP-SO
Fort Sam Houston, TX 78234-6000

U. S. Army Research Institute
Aviation R&D Activity
ATTN: PERI-IR
Fort Rucker, AL 36362

Commander
U.S. Army Safety Center
Fort Rucker, AL 36362

U.S. Army Aircraft Development
Test Activity
ATTN: STEBG-MP-P
Cairns Army Air Field
Fort Rucker, AL 36362

Commander
USAMRDALC
ATTN: SGRD-PLC (COL R. Gifford)
Fort Detrick, Frederick, MD 21702

TRADOC Aviation LO
Unit 21551, Box A-209-A
APO AE 09777

Netherlands Army Liaison Office
Building 602
Fort Rucker, AL 36362

British Army Liaison Office
Building 602
Fort Rucker, AL 36362

Italian Army Liaison Office
Building 602
Fort Rucker, AL 36362

Directorate of Training Development
Building 502
Fort Rucker, AL 36362

Chief
USAHEL/USAAVNC Field Office
P. O. Box 716
Fort Rucker, AL 36362-5349

Commander, U.S. Army Aviation Center
and Fort Rucker
ATTN: ATZQ-CG
Fort Rucker, AL 36362

Chief
Test & Evaluation Coordinating Board
Cairns Army Air Field
Fort Rucker, AL 36362

Canadian Army Liaison Office
Building 602
Fort Rucker, AL 36362

German Army Liaison Office
Building 602
Fort Rucker, AL 36362

French Army Liaison Office
USAAVNC (Building 602)
Fort Rucker, AL 36362-5021

Australian Army Liaison Office
Building 602
Fort Rucker, AL 36362

Dr. Garrison Rapmund
6 Burning Tree Court
Bethesda, MD 20817

Commandant, Royal Air Force
Institute of Aviation Medicine
Farnborough, Hampshire GU14 6SZ UK

Defense Technical Information
Cameron Station, Building 5
Alexandria, VA 22304-6145

Commander, U.S. Army Foreign Science
and Technology Center
AIFRTA (Davis)
220 7th Street, NE
Charlottesville, VA 22901-5396

Commander
Applied Technology Laboratory
USARTL-ATCOM
ATTN: Library, Building 401
Fort Eustis, VA 23604

Commander, U.S. Air Force
Development Test Center
101 West D Avenue, Suite 117
Eglin Air Force Base, FL 32542-5495

Aviation Medicine Clinic
TMC #22, SAAF
Fort Bragg, NC 28305

Dr. H. Dix Christensen
Bio-Medical Science Building, Room 753
Post Office Box 26901
Oklahoma City, OK 73190

Commander, U.S. Army Missile
Command
Redstone Scientific Information Center
ATTN: AMSMI-RD-CS-R
/ILL Documents
Redstone Arsenal, AL 35898

Director
Army Personnel Research Establishment
Farnborough, Hants GU14 6SZ UK

U.S. Army Research and Technology
Laboratories (AVSCOM)
Propulsion Laboratory MS 302-2
NASA Lewis Research Center
Cleveland, OH 44135

Commander
USAMRDALC
ATTN: SGRD-ZC (COL John F. Glenn)
Fort Detrick, Frederick, MD 21702-5012

Dr. Eugene S. Channing
166 Baughman's Lane
Frederick, MD 21702-4083

U.S. Army Medical Department
and School
USAMRDALC Liaison
ATTN: HSMC-FR
Fort Sam Houston, TX 78234

Dr. A. Kornfield, President
Biosearch Company
3016 Revere Road
Drexel Hill, PA 29026

NVESD
AMSEL-RD-NV-ASID-PST
(Attn: Trang Bui)
10221 Burbeck Road
Fort Belvoir, VA 22060-5806

CA Av Med
HQ DAAC
Middle Wallop
Stockbridge, Hants S020 8DY UK

Director
Federal Aviation Administration
FAA Technical Center
Atlantic City, NJ 08405

Commander, U.S. Army Test
and Evaluation Command
ATTN: AMSTE-AD-H
Aberdeen Proving Ground, MD 21005

Naval Air Systems Command
Technical Air Library 950D
Room 278, Jefferson Plaza II
Department of the Navy
Washington, DC 20361

Director
U.S. Army Ballistic
Research Laboratory
ATTN: DRXBR-OD-ST Tech Reports
Aberdeen Proving Ground, MD 21005

Commander
U.S. Army Medical Research
Institute of Chemical Defense
ATTN: SGRD-UV-AO
Aberdeen Proving Ground,
MD 21010-5425

Commander
USAMRDALC
ATTN: SGRD-RMS
Fort Detrick, Frederick, MD 21702-5012

Director
Walter Reed Army Institute of Research
Washington, DC 20307-5100

HQ DA (DASG-PSP-O)
5109 Leesburg Pike
Falls Church, VA 22041-3258

Harry Diamond Laboratories
ATTN: Technical Information Branch
2800 Powder Mill Road
Adelphi, MD 20783-1197

U.S. Army Materiel Systems
Analysis Agency
ATTN: AMXSY-PA (Reports Processing)
Aberdeen Proving Ground
MD 21005-5071

U.S. Army Ordnance C
and School Library
Simpson Hall, Building 3071
Aberdeen Proving Ground, MD 21005

U.S. Army Environmental
Hygiene Agency
ATTN: HSHB-MO-A
Aberdeen Proving Ground, MD 21010

Technical Library Chemical Research
and Development Center
Aberdeen Proving Ground, MD
21010-5423

Commander
U.S. Army Medical Research
Institute of Infectious Disease
ATTN: SGRD-UIZ-C
Fort Detrick, Frederick, MD 21702

Director, Biological
Sciences Division
Office of Naval Research
600 North Quincy Street
Arlington, VA 22217

Commander
U.S. Army Materiel Command
ATTN: AMCDE-XS
5001 Eisenhower Avenue
Alexandria, VA 22333

Commandant
U.S. Army Aviation
Logistics School ATTN: ATSQ-TDN
Fort Eustis, VA 23604

Headquarters (ATMD)
U.S. Army Training
and Doctrine Command
ATTN: ATBO-M
Fort Monroe, VA 23651

IAF Liaison Officer for Safety
USAF Safety Agency/SEFF
9750 Avenue G, SE
Kirtland Air Force Base
NM 87117-5671

Naval Aerospace Medical
Institute Library
Building 1953, Code 03L
Pensacola, FL 32508-5600

Command Surgeon
HQ USCENTCOM (CCSG)
U.S. Central Command
MacDill Air Force Base, FL 33608

Air University Library
(AUL/LSE)
Maxwell Air Force Base, AL 36112

U.S. Air Force Institute
of Technology (AFIT/LDEE)
Building 640, Area B
Wright-Patterson
Air Force Base, OH 45433

Henry L. Taylor
Director, Institute of Aviation
University of Illinois-Willard Airport
Savoy, IL 61874

Chief, National Guard Bureau
ATTN: NGB-ARS
Arlington Hall Station
111 South George Mason Drive
Arlington, VA 22204-1382

Commander
U.S. Army Aviation and Troop Command
ATTN: AMSAT-R-ES
4300 Goodfellow Bouvelard
St. Louis, MO 63120-1798

U.S. Army Aviation and Troop Command
Library and Information Center Branch
ATTN: AMSAV-DIL
4300 Goodfellow Boulevard
St. Louis, MO 63120

Federal Aviation Administration
Civil Aeromedical Institute
Library AAM-400A
P.O. Box 25082
Oklahoma City, OK 73125

Commander
U.S. Army Medical Department
and School
ATTN: Library
Fort Sam Houston, TX 78234

Commander
U.S. Army Institute of Surgical Research
ATTN: SGRD-USM
Fort Sam Houston, TX 78234-6200

AAMRL/HEX
Wright-Patterson
Air Force Base, OH 45433

Product Manager
Aviation Life Support Equipment
ATTN: AMCPM-ALSE
4300 Goodfellow Boulevard
St. Louis, MO 63120-1798

Commander and Director
USAE Waterways Experiment Station
ATTN: CEWES-IM-MI-R,
CD Department
3909 Halls Ferry Road
Vicksburg, MS 39180-6199

Commanding Officer
Naval Biodynamics Laboratory
P.O. Box 24907
New Orleans, LA 70189-0407

Assistant Commandant
U.S. Army Field Artillery School
ATTN: Morris Swott Technical Library
Fort Sill, OK 73503-0312

Mr. Peter Seib
Human Engineering Crew Station
Box 266
Westland Helicopters Limited
Yeovil, Somerset BA20 2YB UK

U.S. Army Dugway Proving Ground
Technical Library, Building 5330
Dugway, UT 84022

U.S. Army Yuma Proving Ground
Technical Library
Yuma, AZ 85364

AFFTC Technical Library
6510 TW/TSTL
Edwards Air Force Base,
CA 93523-5000

Commander
Code 3431
Naval Weapons Center
China Lake, CA 93555

Aeromechanics Laboratory
U.S. Army Research and Technical Labs
Ames Research Center, M/S 215-1
Moffett Field, CA 94035

Sixth U.S. Army
ATTN: SMA
Presidio of San Francisco, CA 94129

Commander
U.S. Army Aeromedical Center
Fort Rucker, AL 36362

Strughold Aeromedical Library
Document Service Section
2511 Kennedy Circle
Brooks Air Force Base, TX 78235-5122

Dr. Diane Damos
Department of Human Factors
ISSM, USC
Los Angeles, CA 90089-0021

U.S. Army White Sands
Missile Range
ATTN: STEWS-IM-ST
White Sands Missile Range, NM 88002

U.S. Army Aviation Engineering
Flight Activity
ATTN: SAVTE-M (Tech Lib) Stop 217
Edwards Air Force Base, CA 93523-5000

Ms. Sandra G. Hart
Ames Research Center
MS 262-3
Moffett Field, CA 94035

Dr. Christine Schlichting
Behavioral Sciences Department
Box 900, NAVUBASE NLON
Groton, CT 06349-5900

Commander, HQ AAC/SGPA
Aerospace Medicine Branch
162 Dodd Boulevard, Suite 100
Langley Air Force Base,
VA 23665-1995

Commander
Aviation Applied Technology Directorate
ATTN: AMSAT-R-T
Fort Eustis, VA 23604-5577

Director
Aviation Research, Development
and Engineering Center
ATTN: AMSAT-R-Z
4300 Goodfellow Boulevard
St. Louis, MO 63120-1798

Commander
USAMRDALC
ATTN: SGRD-ZB (COL C. Fred Tyner)
Fort Detrick, Frederick, MD 21702-5012

Director
Directorate of Combat Developments
ATTN: ATZQ-CD
Building 515
Fort Rucker, AL 36362